$n = 2$, the sensitivity to roll position is markedly reduced; and, finally, for $n \geqq 3$, the pressure becomes independent of the roll position at all angles of attack.

Conclusion

A closed-form equation is obtained which describes the average pressure acting at n equally-spaced points located around the circumference of a body of revolution with an angle of attack in hypersonic flow. It is found that when $n \geqq 3$, the average normalized pressure depends only upon the local body slope and the total angle of attack, and is independent of both the aerodynamic roll angle and the number of points.

References

[1] Potter, J. L., Kinslow, M., and Boylan, D. E., "An Influence of the Orifice on Measured Pressures in Rarefied Flow," *Rarefied Gas Dynamics*, Supplement 3, Vol. II, Academic Press, New York, 1966, pp. 175–194.

[2] Bartz, J. A. and Vidal, R. J., "Experimental Study of Pseudo Transpiration at an Orifice in Rarefied Flow," *Rarefied Gas Dynamics*, Supplement 5, Vol. I, edited by Trilling and Wachman, Academic Press, New York, 1969, pp. 639–653.

[3] Kienappel, K., "Inclination of Pressure Orifices in Low-Density Flow," *AIAA Journal*, Vol. 9, No. 4, April 1971, pp. 749–750.

[4] Bennett, M. D., "Shock-Wave Boundary-Layer Interaction on a Missile Nose Probe," *AIAA Journal*, Vol. 1, No. 8, August 1963, pp. 1938–1940.

[5] Truitt, R. W., *Hypersonic Aerodynamics*, Ronald Press, New York, 1959, pp. 71.

A Finite-Difference Method for Boundary Layers with Reverse Flow

M. J. WERLE* AND S. D. BERTKE†
University of Cincinnati, Cincinnati, Ohio

BOUNDARY LAYER separation occurs in virtually all aerodynamic flight regimes. Although interest in the details of this flow problem has existed for several decades, quantitative estimates based on numerical solutions of the governing equations have only recently been documented[1] where here the principal difficulty encountered is reported to be the presence of reverse flow. Since this, in effect, delivers information from a downstream point, it is identified with several numerical instabilities observed when one attempts to use a numerical finite-difference scheme to march into a separation bubble. Although this may certainly be true, it is also interesting to note that solutions of the self-similar form of the governing equations, which do not contain the convective terms believed to be causing numerical difficulties, also suffer numerical instabilities when finite-difference methods are applied to their solution. In particular, it is found that attempts to recover Stewartson's[2] reverse flow profiles for the Falkner-Skan[3] equation using finite differences fail, and only the forward profile solution is recovered. Only the shooting techniques[4,5] have thus far been able to overcome this deficiency. Unfortunately, shooting techniques have not yet been successfully carried over to nonsimilar boundary-layer calculations and, in fact, are found to be rather tedious to apply for the self-similar cases.

The present works demonstrates the application of a finite-difference technique that readily recovers Stewartson's reverse flow profiles without difficulty. The tedium of shooting methods is eliminated and the present method is shown to be reasonably fast and very insensitive to errors in initial data, overcoming up to a 30% error (purposely introduced) to recover the exact solution. It is anticipated that this method will be helpful in overcoming some of the difficulties presently being encountered in nonsimilar boundary-layer separation studies, and in any boundary-layer problem with nonunique solutions.

Received February 25, 1972. This research was supported by the Naval Air Systems Command, Air 320 under Contract N00019-72-C-0136.

Index category: Boundary Layers and Convective Heat Transfer—Laminar.

* Associate Professor of Aerospace Engineering. Member AIAA.
† Graduate Student, Department of Aerospace Engineering.

Solution of the Governing Equations

The Falkner-Skan equations can be written in Görtler variables as two equations

$$F_{\eta\eta} - VF_\eta + \beta(1 - F^2) = 0 \tag{1a}$$

$$F + V_\eta = 0 \tag{1b}$$

where the pressure-gradient parameter is

$$\beta = (2\xi/u_e)(du_e/d\xi) \tag{2}$$

and the boundary conditions are

$$F(0) = V(0) = 0 \tag{3a}$$

and

$$F(\infty) = 1 \tag{3b}$$

Note that in this form, Eq. (1a) represents a transformed version of the momentum equation with F a normalized longitudinal velocity, and Eq. (1b) gives the continuity equation, with V related to the velocity normal to the surface. The variables monitored in the present study are the wall stress, given by

$$\tau_w = (\partial F/\partial\eta)_w \tag{4}$$

and a transformed displacement thickness, defined by

$$\delta \equiv \int_0^\infty (1 - F)d_\eta \tag{5}$$

In the preceding equations for $\beta \geqq 0$, accelerated flow and unique solutions result, while for $-0.19884 \leqq \beta \leqq 0$, a nonuniqueness is encountered. In this case, there are an infinite number of solutions of the governing equations, but only two are acceptable in that they have an exponential approach to the outer boundary conditions. These are the usual forward flow profiles of Falkner and Skan[3] and the reversed flow solutions, first identified by Stewartson.[2]

To recover these latter solutions, note first that the continuity equation and boundary conditions imply that

$$V \rightarrow -\eta + \delta \text{ as } \eta \rightarrow \infty \tag{6}$$

This result can be used to obtain numerical solutions to the continuity equation for any given value of δ, since an integration of Eq. (1b) could proceed inward from the outer edge, η_e. However, it is found numerically that only two such solutions satisfy the boundary condition $V_w = V(0)$. This is demonstrated in Fig. 1, where the value of V_w is given as a function of δ for $\beta = -0.18$. These latter solutions were obtained from fiinite-difference solutions of Eqs. (1–3) with $V(0) = 0$ replaced with Eq. (6) at some large $\eta = \eta_{edge}$.

As one might suspect the lower value of δ corresponds to the attached flow solution, whereas the reverse flow solution is given by the larger displacement thickness. The solution technique used here works in the V_w vs δ plane and, simply stated, uses a reverse integration of the continuity equation to identify the largest value of δ which gives $V_w = 0$.

To solve this problem numerically, first denote the exact solutions of the governing equations as F and V, and corresponding trial solutions as F_G and V_G the relations between these values being written as

$$V = V_G + v \tag{7a}$$

$$F = F_G + f \tag{7b}$$

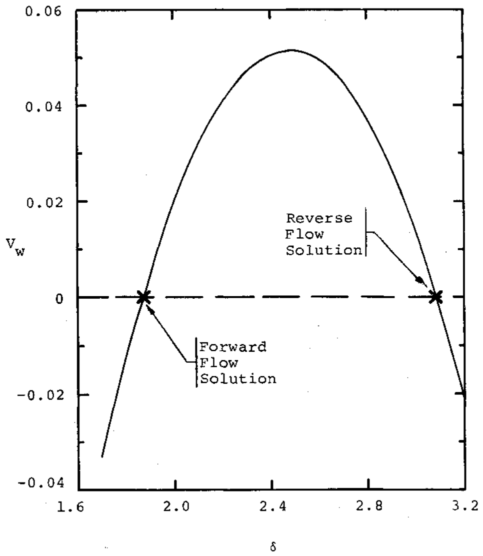

Fig. 1 Wall velocity dependence on delta.

where v and f are errors that become small as the trial values approach the true solution. Substituting Eq. (7) into (1a), and neglecting quadratic terms in f and v, a quasi-linearized form of the momentum equation is obtained as

$$F_{\eta\eta} - V_G F_\eta - (2\beta F_G)\cdot F + (\beta + V_G F_{G\eta} + \beta F_G^2) - (F_{G\eta})\cdot V = 0 \tag{8}$$

The derivatives in Eq. (8) can be replaced by second-order central-difference approximations, resulting in

$$A_n F_{n-1} + B_n F_n + C_n F_{n+1} = D_n - E_n V_n \tag{9}$$

where the coefficients are given by

$$A_n = (2 + V_G\Delta)/2\Delta^2 \tag{10a}$$

$$B_n = -2(1/\Delta^2 + \beta F_G) \tag{10b}$$

$$C_n = (2 - V_G\Delta)/2\Delta^2 \tag{10c}$$

$$D_n = -\beta(1 + F_G{}^2) + V_G E_n \tag{10d}$$

$$E_n = -(F_{G,n+1} - F_{G,n-1})/2\Delta \tag{10e}$$

and Δ is the η-mesh width. The solution of Eq. (9) can be written as‡

$$F_n = \tilde{E}_n F_{n+1} + \tilde{F}_n + \tilde{G}_n V_{n+1} \tag{11}$$

where

$$\tilde{E}_n = -\frac{C_n + (\Delta/2)(A_n\tilde{G}_{n-1} + E_n)}{[A_n\tilde{E}_{n-1} + B_n + (\Delta/2)(A_n\tilde{G}_{n-1} + E_n)]} \tag{12a}$$

$$\tilde{F}_n = \frac{D_n - A_n\tilde{F}_{n-1}}{[A_n\tilde{E}_{n-1} + B_n + (\Delta/2)(A_n\tilde{G}_{n-1} + E_n)]} \tag{12b}$$

$$\tilde{G}_n = -\frac{A_n\tilde{G}_{n-1} + E_n}{[A_n\tilde{E}_{n-1} + B_n + (\Delta/2)(A_n\tilde{G}_{n-1} + E_n)]} \tag{12c}$$

The boundary conditions applicable to the momentum recursion relation are

$$F_n = 1 \text{ at the edge } \eta_n = N\Delta, \tag{13}$$

and

$$F_1 = 0 \text{ at the wall } \eta = 0 \tag{14}$$

which translates to the condition that

$$\tilde{E}_1 = \tilde{F}_1 = \tilde{G}_1 = 0 \tag{15}$$

To complete the solution, the continuity equation is integrated inward from the outer edge using a trapezoid rule, to give

$$V_n = V_{n+1} + (F_{n+1} + F_n)/2\Delta \tag{16}$$

‡ The authors are indebted to R. T. Davis of the University of Cincinnati, and Kaiser and Mook of Virginia Polytechnic Institute for introducing them to and working out the details of this approach to solving the boundary-layer equations.

Here, the integration is started at the point $n = N$, employing the boundary condition

$$V_n = -\eta_n + \delta_G \tag{17}$$

with the correct solution obtained for a δ_G that produces $V_1 = 0$.

Solutions of the above set of equations were obtained for a given β and δ_G iteratively, by relaxing an initial guess on F_G and V_G until no significant changes in the profile were observed. This provided a single point on the equivalent to Fig. 1.

A second value of δ_G produced another such point, and thereafter a Newton-Raphson scheme was applied to find the intercept point on the δ axis.

Results and Discussion

All of the present calculations were performed on an IBM 360-65 computer, using double-precision arithmetic throughout. Solutions were first obtained by incrementing β slightly from the separation value and marching towards $\beta = 0$.

The resulting values of wall stress, τ_w, agree to at least three significant figures with the results of Christian, Hankey and Petty[4] obtained using a shooting technique to integrate the governing equations. The velocity profiles showed the same order of agreement. The shear stresses and displacement thicknesses so obtained for both forward and reversed flow are shown in Fig. 2. The entire lower branch corresponding to 19 reverse flow profiles required approximately 3.3 min of computer time. The upper branch of the δ curve, again corresponding to reversed flow, shows a rapid increase in δ as $\beta \to 0$. In the computations, proper convergence of the profile was not obtained unless η_N was adjusted to be significantly larger than the anticipated value of δ.

A second set of calculations was performed to test the sensivity of the present technique to input errors, since Petty[6] and others have noted that the shooting technique is extremely sensitive to errors in the initial guesses. A series of runs were performed with F_G initialized at unity and V_G at $-\eta + \delta_G$ across the boundary layer for set errors in the values of δ_G. The results are shown in Table 1. It should be noted that about 8 sec of the stated computer times (about 16 iterations) were required to adjust the guessed values of F to convergence, even when the exact value

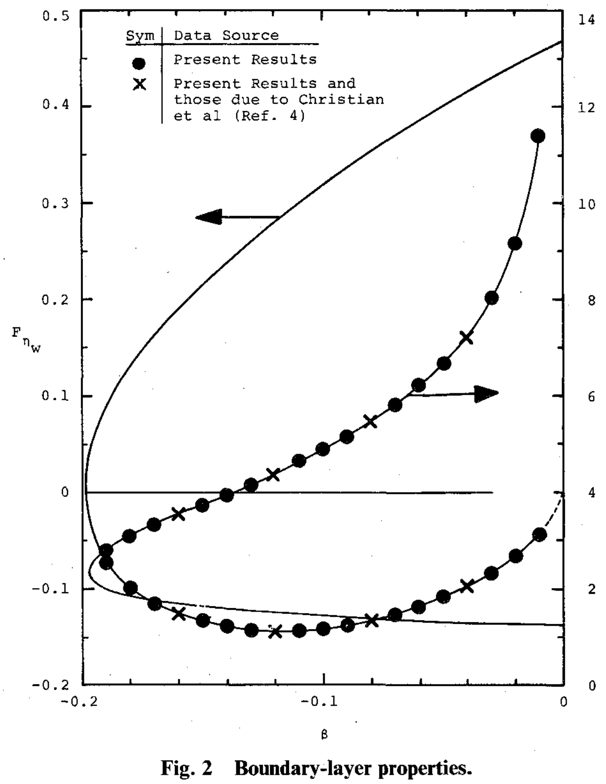

Fig. 2 Boundary-layer properties.

of δ was used to initialize computations. Thus, further acceleration of the technique could easily be achieved taking better initial values of F_G and V_G. Table 1 shows that the time (or number of iterations) rises only slightly for initial δ guesses as much as $\pm 30\%$ in error. Below a certain δ value, the process converges to the positive-flow case rapidly (as shown by Fig 1). In some cases, a guess of 50% to 100% high on δ was found to still converge to the reversed-flow profile. Thus, compared to the usual shooting technique (where an initial boundary condition is guessed), this process is relatively insensitive to initialization and can be made to converge quickly to either solution branch.

Table 1 Input error influence on iteration scheme

β	Time for convergence, sec					
	δ input error					
	+10%	−10%	+20%	−20%	+30%	−30%
−0.04	15	15	16	17	18	27
−0.08	14	13	18	17	14	23

As a final note, it is pointed out that solutions were also obtained to an uncoupled (through V) version of Eqs. (8) and (16). This approach as used by Blottner[1] and others employs a quasilinear version of the momentum equation that only contains V in its guessed state, V_G. This method was also successful for present purposes but it was found that the computer time to convergence was prohibitively large for the reversed-flow cases where $-0.12 \leqq \beta < 0$.

It is believed that the present technique provides a rapid, effective means of solving nonunique boundary-layer problems as applied here to the Falkner-Skan equations. As such it provides a basis for addressing nonsimilar separating boundary-layers where it is anticipated approximations similar to those of Reyhner and Flügge-Lotz[1] will be required to overcome the physical reverse flow instability.

References

1 Reyhner, T. A. and Flügge-Lotz, I., "The Interaction of a Shock Wave with a Laminar Boundary Layer," No. 163, 1966, Div. of Engineering Mechanics, Stanford Univ., Palo Alto, Calif.

2 Stewartson, K., "Further Solutions of the Falkner-Skan Equation," *Proceedings of the Royal Society*, Ser. A, Vol. 312, 1955, pp. 181–206.

3 Falkner, V. M. and Skan, S. W., "Solutions of the Boundary Layer Equations," Philosophical Magazine, Vol. 12, 1931, pp. 865–896.

4 Christian, J. W., Hankey, W. L., and Petty, J. S., "Similar Solutions of the Attached and Separated Compressible Laminar Boundary Layer with Heat Transfer and Pressure Gradiant," Rept. ARL 70-0023, 1970, Aerospace Research Labs., Wright Patterson Air Force Base, Ohio.

5 Rogers, D. F., "Adiabatic Wall Solutions for the Hypersonic Compressible Laminar Boundary-Layer Equations," *The Physics of Fluids*, Vol. 13, 1970, pp. 1142–1145.

6 Petty, J., private communication, 1971.

7 Blottner, F. G., "Finite Difference Methods of Solution of the Boundary-Layer Equations," *AIAA Journal*, Vol. 8, No. 2, Feb. 1970, pp. 183–205.

Approximate Temperature Distribution for a Diffuse, Highly Reflecting Material

KENNETH C. WESTON*
University of Tulsa, Tulsa, Okla.
AND
JOHN T. HOWE† AND MICHAEL J. GREEN‡
NASA Ames Research Center, Moffett Field, Calif.

Nomenclature

B = Biot modulus, $h\delta/K$
h = convective heat-transfer coefficient
I_R = reflecting flux
I_T = transmitted flux
k = Kubelka-Munk absorption coefficient
K = thermal conductivity
q_o = incident radiative heat flux
q_R = radiative heat flux
R = reflectance of material
R_B = reflectance of back surface
R_∞ = reflectance of a slab of infinite thickness
r = I_R/I_T
s = Kubelka-Munk scattering coefficient
S = scattering power, $s\delta$
T = temperature
T_s = stream temperature
u = internal energy
y = coordinate normal to surface of material
δ = slab thickness
η = dimensionless distance, y/δ
θ = nondimensional temperature $(T-T_o)/T_s$
ρ = density
Φ = nondimensional parameter, $kq_o\delta^2/KT_s$

Introduction

IT has been proposed[1] that highly-backscattering materials may provide efficient thermal protection for probes encountering planetary entry environments in which radiative heating is the dominant mode of heat transfer. Radiative transfer in such materials may be studied by use of the equation of radiative transfer as discussed in Chandrasekhar[2] and elsewhere. For engineering purposes however the "two-flux method" is convenient and informative. This approach to radiative transfer has been used by astrophysicists[3] in the paint and paper industry[4,5] and in the analysis of thermal control coatings.[6,7] The present work considers applications of the "two-flux" technique to the reflective characteristics and temperature distribution in highly-scattering materials with vanishingly small absorption coefficient. It is assumed here that internal radiative emission may be neglected with respect to the transmitted internal radiation fields.

Two-Flux Radiation Field

The radiation field is assumed to be governed by the Kubelka-Munk differential equations.[4] These equations describe the diminution of right and leftgoing fluxes I_T and I_R due to scattering

Received March 2, 1972; revision received May 2, 1972. This research has been supported in part under NASA Grant NGR 37-008-003.

Index categories: Heat Conduction; Radiation and Radiative Heat Transfer; Entry Vehicles and Landers.

* Associate Professor of Mechanical-Aerospace Engineering. Member AIAA.

† Research Scientist.

‡ Mathematician.